3 Factors controlling the crustal density structure underneath active continental margins with implications for their evolution

Author: Andrés Tassara

Paper accepted (September 20th, 2005) for publication in *Geochemistry, Geophysics, Geosystems*.

Abstract

The design and interpretation of gravity-based Earth models requires sufficient knowledge of the effect exerted on continental crustal density by chemical composition, pressure-temperature (PT) conditions and water content. This need has motivated the development of a petrophysical modelling for 55 major element analyses compiled to characterize the geochemical differentiation trend of active continental margins. Equilibrium mineral assemblages and densities were computed using two independent thermodynamic approaches along conductive geotherms representing volcanic arcs and shields. Results under anhydrous conditions demonstrate that density is inversely correlated with the weight percent of SiO_2 for all PT conditions. Empirical relationships with correlation factors commonly better than 0.9 allow the density under active continental margins to be estimated from silica content at critical conditions. Calculations for H_2O-saturated systems and estimates of the effect produced by retained melt on the bulk density of lower crustal zones of melting, assimilation, storage and homogenisation (MASH zones), indicate that these empirical relationships should also hold for wet, melt-containing crustal columns of acidic to intermediate composition. They cannot be applied for basic compositions because mafic rocks absorb significant amounts of water via the formation of amphiboles, strongly reducing their density with respect to the dry granulites formed by garnet-pyroxene assemblages. This fact, plus the density reduction generated by the retention of some volume percent of melt, suggests that MASH zones underneath hydrated, subduction-related magmatic arcs thinner than 50 km could contain large amounts of basic to ultrabasic material (SiO_2 as low as 43 wt%) in a gravitationally stable situation. This could have implications for estimates of global crustal composition and models of crustal growth. The results also suggest restricted thermal, compositional and tectonic conditions for the removal of lower crust into the mantle.

3.1. Introduction

Modelling the observed gravity field provides a powerful tool for analysing the three-dimensional mass distribution inside the Earth. However, the design of density models reproducing the gravity field and their interpretation require sufficient knowledge of the density structure of crust and mantle and its dependency on several factors. Such knowledge is also important to improve our understanding of the geodynamic processes affecting active continental margins where continental crust is created and modified [e.g. Rudnick, 1995; Tatsumi, 2000; Carlson et al., 2005]. These processes include the recycling of lower crust into the mantle via delamination or convective instabilities [Kay and Kay, 1993; Houseman and Molnar, 1997; Tatsumi, 2000; Jull and Kelemen, 2001] and hence the evolution of magmatic arcs [Münthener et al., 2001; Ducea, 2002; Zandt et al., 2004] and orogens [Le Pichon et al., 1997; Leech, 2001; Moore and Wiltschko, 2004].

Controls exerted on mantle density by its chemical composition, thermal regime and water content [e.g. Jordan, 1988; Poudjom Djomani et al., 2001; Kelly et al., 2003; Hacker et al., 2003a; Iwamori, 2004; Lee et al., 2005] are paradoxically better constrained than those affecting the continental crust. This is primarily because the continental crust is strongly heterogeneous, having a wide range of chemical compositions and a complex tectonic structure. The inaccessibility of the lower crust masks its nature and, therefore, knowledge of its compositional structure is mainly derived from models based on indirect observables like seismic velocities and surface heat flow [e.g. Rudnick, 1995; Rudnick and Fountain, 1995; Christensen and Mooney, 1995; McLennan and Taylor, 1996].

Petrophysical modelling, defined by Sobolev and Babeyko [1994] as the direct calculation of physical properties of rocks from their bulk composition and pressure-temperature (PT) conditions of metamorphism, is becoming widely used as a tool to provide petrological meaning to geophysical images [e.g. Hacker et al., 2000; Connolly and Kerrick, 2002; Behn and Kelemen, 2003; Mechie et al., 2004]. This approach has also been used to estimate crustal densities under specific conditions, leading to a better perception of the dynamic processes affecting the lower crust [e.g. Bousquet et al., 1997; Le Pichon et al., 1997; Jull and Kelemen, 2001; Lucassen et al., 2001; Müntener et al., 2001; Ducea, 2002]. Nevertheless, the potential that these techniques have for revealing valuable information on the factors controlling the density of crustal rocks, has not yet been systematically tested.

This manuscript presents a quantitative petrophysical analysis relating the density of crustal materials to its major element composition, water content and PT conditions of equilibration. Fifty-five geochemical analyses were compiled to characterize the

compositional structure beneath an active continental margin and to be used as input for thermodynamic modelling based on the approaches of Sobolev and Babeyko [1994] (S. Sobolev and A. Babeyko, pers. comm. 2004; hereafter SB) and Perple_X [Connolly, 1990] (www.perplex.ethz.ch; hereafter PX). Comparing results obtained by both methods for six compositions representative of the dataset under anhydrous conditions provides an independent estimate of the reliability of these modelling techniques. Results produced by SB for the entire dataset under anhydrous conditions were used to derive empirical relationships between density and silica content at some critical depths. PX was then applied under H_2O-saturated conditions for three compositions characteristic of the lower crust. A linear parameterisation helps to evaluate the effect of retained melt in reducing the density of the lower crust along magmatic arcs.

These results are used to discuss the relative influence of the analysed factors in controlling the density of crustal columns and the implications they could have for models dealing with the composition of the continental crust, its structure and evolution.

3.2. Major element geochemistry of the dataset

In order to characterize the geochemical spectrum of magmatic arcs, 55 major element compositional analyses were compiled from the literature (Fig. 3.1). Acidic to intermediate compositions (74 > wt% SiO_2 > 52) correspond to Palaeo-Mesozoic igneous and meta-igneous rocks outcropping along the Andean continental margin [Parada et al., 1988; Mpodozis and Kay, 1992; Vujovich and Kay, 1998; Rapela et al., 1998; Pankhurst et al., 1998; Sato et al., 2000; Lucassen et al., 2001]. Basic to ultrabasic compositions (52 > wt% SiO_2 > 43] were selected from lower crustal xenoliths [Kay and Abbruzzi, 1996; Pankhurst and Rapela, 1995; Hickey-Vargas et al., 1995; Costa et al., 2002; Ducea, 2002], exposed lower crustal sections [Grisson et al., 1991; Jull and Kelemen, 2001 and reference therein], differentiation models of Andean volcanic suites [Kay et al., 1991; Lopez-Escobar et al., 1995], cumulates generated by fractional crystallization of basalt to andesite experimental liquids [Münthener et al., 2001] and global lower crustal compositions [Rudnick and Fountain, 1995; Behn and Kelemen, 2003 and reference therein].

Although the amount of studied samples is relatively small, they spread along the broad compositional range expected for active continental margins. Figs. 3.1a and 3.1b show that the dataset defines the typical subalkaline signature of magmatic arcs with most of the samples lying in the calcalkaline field. Ultrabasic compositions are mostly tholeitic.

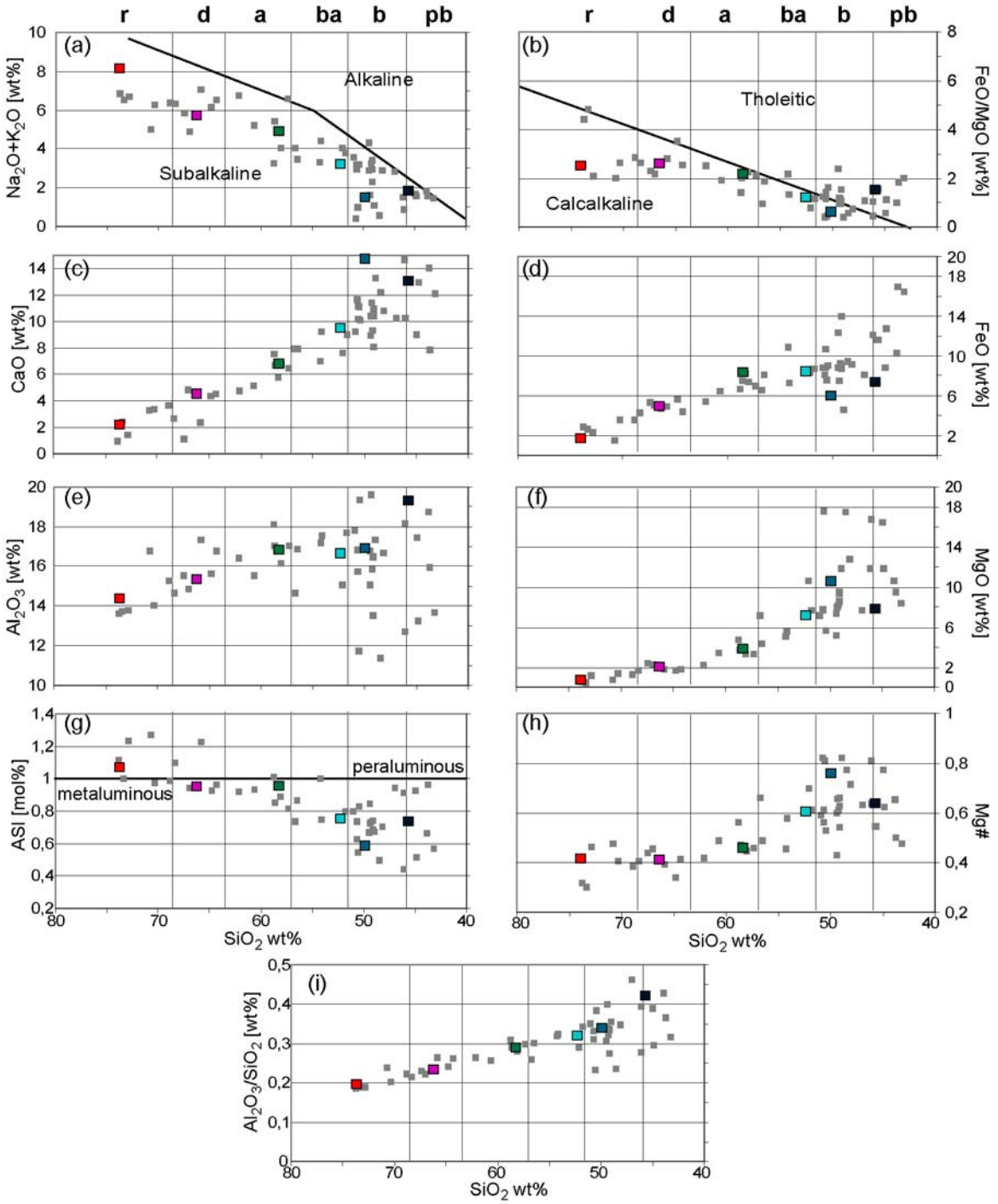

Fig. 3.1. Diagrams showing variations of major oxides (all in weight percent) and petrological indicators against wt% SiO_2 in the x-axis for the 55 compositional analyses forming the studied dataset. r = rhyolite, d = dacite, a = andesite, ba = basaltic andesite, b = basalt, pb = picro-basalt. Note that silica content decreases from left (rhyolite) to right (picro-basalt) because that is the direction in which density increases in following figures. Large coloured symbols are samples used during the extensive petrophysical modelling, the results of which are presented in Fig. 3.2. See table 1 for compositional analyses of these selected samples. (a) Alkalis concentration (Na_2O+K_2O) together with alkaline and subalkaline fields after Rickwood [1989]; the dataset lie in the latter field. (b) FeO/MgO with tholeitic and calcalkaline fields after Miyashiro [1974]; basalts commonly lay in the former field and more evolved samples do it in the latter. (c), (d), (e) and (f) show respectively CaO, FeO, Al_2O_3 and MgO; these oxides are strongly coupled with silica in the intermediate to acidic compositional range, whereas for more basic compositions, a large dispersion occurs mainly in (e) and (f). (g) Aluminium Saturation Index (ASI = $Al_2O_3/CaO+Na_2O+K_2O$, in molar percent) with per- and metaluminous fields as used by Lucassen et al. [2004]; only some rhyolites and dacites are peraluminous. (h) Magnesium number (Mg# =

MgO/MgO+FeO, in molar percent); basic compositions have values between 0.42 and 0.82. (i) Al_2O_3/SiO_2; basic compositions have values between 0.22 and 0.48.

Hereafter compositional ranges are referred for simplicity by the name of their corresponding volcanic equivalents (see Fig. 3.1). Figs. 3.1a to 3.1f show that variations of major elements between basaltic andesite and rhyolite are strongly coupled with that of silica; the database defines a differentiation trend characteristic of those generated in magmatic arcs via fractional crystallization (or partial melting) from a magma (or protolith) with basalt to basaltic andesitic composition [e.g. Grove et al., 2003]. These processes leave mafic residues (in the general sense of Ducea [2002]) that in diagrams of Fig. 3.1 show great dispersion of major element concentrations compared to more acidic compositions. This dispersion is likely to reflect the diverse nature of residual mineral assemblages being formed at lower crustal zones of melting, assimilation, storage and hybridisation (MASH zones after Hildreth and Moobarth [1988]). In particular, picro-basalts having high aluminium saturation indexes (ASI, Fig. 3.1g) and "normal" magnesium numbers (Mg#, Fig. 3.1h) are Andean xenoliths [Pankhurst and Rapela, 1995, Costa et al., 2002] and exposed mafic terrains [references in Jull and Kelemen, 2001] containing hydrated phases, whereas those showing low ASI and high Mg# are anhydrous pyroxenites carried up to the surface by extension-related Miocene lavas from the central Sierra Nevada [Ducea, 2002].

Table 1. Major element geochemistry of samples selected for extensive petrophysical modelling.

wt%	rhyolite[e]	dacite	andesite	basalt.-andesite	basalt	picro-basalt
SiO_2	73,69	66,29	58,3	52,30	49,9	45,60
Al_2O_3	13,57	15,35	16,8	16,60	16,89	19,26
FeO[a]	2,76	4,65	8,1	8,40	6,00	11,53
MgO	0,50	1,80	3,8	7,10	10,50	7,69
CaO	2,17	4,45	5,7	9,40	14,60	12,88
Na_2O	2,56	3,17	3,4	2,60	1,50	1,74
K_2O	4,26	2,57	1,55	0,60	0,03	0,07
Total[b]	99,51	98,28	97,65	97,00	99,42	98,77
Mg#[c]	0,24	0,41	0,46	0,60	0,76	0,54
ASI[d]	1,06	0,95	0,95	0,75	0,58	0,73
Al_2O_3/SiO_2	0,18	0,23	0,29	0,32	0,34	0,42

[a]All iron as Fe^{2+}.
[b]These seven major elements account for more than 97 wt% of the total for each sample.
[c]Magnesium number (see caption of Fig. 3.1 for definition).
[d]Aluminium Saturation Index (see caption of Fig. 3.1 for definition).
[e]See text for references from which each compositional analysis was selected.

Six samples were selected to perform an extensive petrophysical modelling (see Fig. 3.1 and Table 1). The rhyolite is a coarse-grained leucocratic granite representative of the acidic Late Palaeozoic magmatism occurred along the western margin of Gondwana [Mpodozis and Kay, 1992]. The dacite is a medium-grained hornblende-biotite granodiorite formed in an Ordovician continental magmatic arc currently exhumed along the Argentinean Pampean Ranges [Pankhurst et al., 1998]. The andesite is the average of granulitic terrains with intermediate compositions compiled by Rudnick and Fountain [1995]. The basaltic andesite is the composition proposed by the same authors as representative of the lower continental crust worldwide. The basalt is a gabbro exposed in the Oman ophilitic complex and the picro-basalt is a gabbronorite outcropping in the Alaskan Tonsina arc section. These two rocks were used by Jull and Kelemen [2001] to characterize residues left at the base of magmatic arcs. Note that in the diagrams of Fig. 3.1, the selected samples with compositions between rhyolite and basaltic andesite have concentrations of major elements and elemental ratios lying in the middle of the differentiation trend. The basalt is somehow anomalous within the disperse basic compositional range, having low ASI, high Mg# und very high CaO concentration. The picro-basalt has normal values of ASI and Mg# but the total concentration of Al_2O_3 and FeO+MgO are respectively very high and very low.

3.3. Petrophysical modelling

Compositional analyses are used as the input to calculate the mineral assemblage (i.e. volume percent of stable mineral phases) that minimizes the free energy contained in the thermodynamic system at various PT conditions of equilibration. The thermodynamic system is here defined by the weight percent of the major oxides SiO_2, Al_2O_3, FeO, MgO, CaO, Na_2O, K_2O, which account for more than 97% of the composition of each selected sample (Table 1). Pressures used in this study were extracted from a lithostatic gradient for an average density of 3 Mg/m^3. Considering a variation of ±0.2 Mg/m^3, an uncertainty of ±0.1 GPa (~5%) characterizes pressure values at 60 km depth. Temperatures were calculated along conductive geotherms of the form:

$$T(z) = Ts + \frac{Qs - \rho Hl}{k} z + \frac{\rho H l^2}{k}(1 - e^{-z/l})$$

where z is depth, Ts = 25°C is surface temperature, ρ = 3 Mg/m^3 is average density, H = 1.1 μW/m^3 is crustal heat productivity [Rudnick and Fountain, 1995], l = 10 km is the length

scale for the decrease of H with depth and k = 2.5 W/m°C is thermal conductivity [Turcotte and Schubert, 2002, p.147]. With this parameterisation, the 1D thermal structure of the continental lithosphere depends exclusively on the surface heat flow density *Qs*. Common variance in *Qs* (±5 mW/m^2), k (±0.5 mW/m2) and H (±0.3 μW/m^3) lead to a temperature uncertainty of ±200°C (~20%) at 60 km depth.

Two extreme thermal situations were explored; a cold geotherm representing shield conditions with a surface heat flow of 45 mW/m^2 and a hot thermal gradient characterising volcanic arcs with a surface heat flow of 80 mW/m^2. A conductive gradient for an active volcanic arc probably underestimates crustal temperatures because it neglects the likely relevant thermal effect of magmatic advection, but simplifies the method and allows a direct comparison with results produced for conductively cooled cratonic regimes.

The modelling methods of Sobolev and Babeyko [1994, SB] and Perple_X [Connolly 1990, PX] are based on similar algorithms to find the equilibrium mineral assemblages that minimize the total Gibbs (free) energy contained in the thermodynamic system for a given PT condition, but on different data for the thermochemical and physical properties of mineral phases. SB uses a database for anhydrous minerals optimised for crustal and upper mantle conditions [Sobolev and Babeyko, 1994], whereas the version of PX applied here uses the most recent update (March 2004) of the Holland and Powell [1998] database, which includes properties of anhydrous as well as hydrous minerals. Results presented below indicate that difference in phase proportions and densities calculated by both approaches under the same thermodynamic conditions are generally lower than those generated by uncertainties in temperatures. However, some important differences persist for andesite and basaltic andesite compositions that justify a comparison of the results generated by both methods.

Equilibrium mineral assemblages formed under anhydrous conditions were calculated using both approaches along hot and cold geotherms but for temperatures higher than 700°C, the temperature threshold below which reaction velocities are supposed to be too slow for equilibrium to be achieved on geological time-scales [e.g. Hacker, 1996; Le Pichon et al., 1997; Austrheim, 1998; Bjornerud and Austrheim, 2004]. For H_2O-saturated conditions performed with PX, this “kinetic barrier” was reduced to 500°C because low-temperature chemical reactions could be catalysed by fluids [e.g. Leech, 2001 and reference therein].

The bulk density of the obtained mineral assemblages was then computed for *in situ* PT conditions from the calculated volume proportion of stable phases and normative density (i.e. at room PT conditions), expansion coefficient and compressibility values contained in the databases used by each of the methods. For depths shallower than the one at which the

thermal kinetic barrier is reached (hereafter “kb-depth”), densities were calculated for mineral assemblage equilibrated at temperatures corresponding to this barrier and pressures at *in situ* conditions, but taking into account the thermal compression suffered by the assemblage because temperatures along the conductive gradient are lower than this barrier.

3.4. Results

3.4.1. Anhydrous crust

Density profiles and mineral assemblages calculated under dry conditions for the six samples selected to perform an extensive analysis (Table 1 and Fig. 3.1) are presented in Fig 3.2a and 3.2b. For each composition, Fig. 3.2a shows the density range constrained by profiles computed along hot and cold geothermal gradients for depths between 0 and 70 km. The kinetic barrier of 700°C is intersected by the hot geotherm at 32 km depth (Fig. 3.2b) but this barrier is always higher than temperatures along the cold geotherm. Fig. 3.2b shows the explored geotherms and mineral assemblages estimated by both methods for rhyolite, andesite, basaltic andesite and picro-basalt compositions at five critical depths. In the following, the terms upper, lower and lowermost crust are respectively used to describe the results for the depth ranges 0-20 km, 20-45 km and 45-70 km. The so-defined lowermost crust corresponds to the lower portion of a tectonically thickened crust. Calculated crustal densities can be compared against a “mantle range” of 3.25 to 3.35 Mg/m^3 (Fig. 3.2a and c), as defined by values reported by several authors for continental mantle lithosphere under diverse thermal regimes [Poudjom Djomani et al., 2001; Jull and Kelemen, 2001; Kelly et al., 2003]. Density difference lower than 1% between those calculated by both approaches or resulting from temperature differences along both geotherms will be considered insignificant compared with the variance introduced by uncertainties in thermochemical and petrophysical data or parameters defining the conductive geotherms.

3.4.1.1. Upper crust

The density of rocks formed by each analysed crustal composition, being almost constant along the upper crustal section, is mainly controlled by their silica content. Density values increase from 2.68 Mg/m^3 for the rhyolite to 3.06 Mg/m^3 for the picro-basalt composition (Fig. 3.2a). A maximum variability of 0.01 Mg/m^3 (0.3%) at 20 km depth results from temperature difference between the cold and hot geotherm of up to 250°C. Irrelevant variations of the same magnitude occurs between densities calculated by both thermodynamic approaches. Constant densities are likely the consequence of two phenomena. First, mineral

assemblages remain unchanged in this pressure-depth range, although the rhyolite forms a granite with garnet contents increasing downward from 0 to 3.5%, explaining the slight density increment with depth. The other three compositions monitored in Fig. 3.2b form orthopyroxene granodiorite, two-pyroxene gabbro and olivine gabbro. Second, the downward thermal expansion experienced by each rock along the *in situ* geotherms is counteracted by the pressure contraction along the lithostatic gradient.

3.4.1.2.Lower crust

Up to the kb-depth, i.e. between 20 and 32 km depth, densities calculated by SB increase with depth for all compositions. However, densities calculated by PX for andesite and basaltic andesite at 32 km depth are ~0.1 Mg/m^3 (~3.3%) lower than those obtained by SB for the same PT conditions. This relevant difference is due to the minor amount of garnet present in PX assemblages respect to those calculated by SB. These discrepancies are likely related to difference either in the thermodynamic data used in each approach or in the models assumed to treat solid solutions, but a detailed analysis on this issue is outside the scope of this work. The discrepancy between SB and PX imposes an important uncertainty to the expected density of rocks with an andesite to basaltic andesite composition along the deep portion of the lower crust. In particular, the density increment of ~5% suggested by SB that could take place between 20 and 35 km depth for these compositions, is estimated to occur below this depth range by PX.

The magnitude of this density increment along the lower crust is inversely correlated with the silica content of each sample, being weak for the rhyolite (0.015 Mg/m^3 = 0.5%) and strong for the picro-basalt (0.3 Mg/m^3 = 9.5%). This latter composition forms an assemblage that surpasses the density of the mantle range (Fig. 3.2a) at depths as shallow as 25 km. For each composition, the density variations caused by 300°C temperature difference between the hot and cold thermal gradient at 32 km depth, are up to 0.03 Mg/m^3 (~1%). The density increment between 20 and 32 km depth, occurring at a constant equilibration temperature of 700°C, is driven by a pressure-controlled change in the mineral assemblages. At 32 km depth (~0.95 GPa), this change is greatest for the picro-basalt composition, for which all the olivine and more than 50% of the plagioclase contained at 20 km depth are consumed to form a mafic granulite with 40% garnet and 32% clinopyroxene.

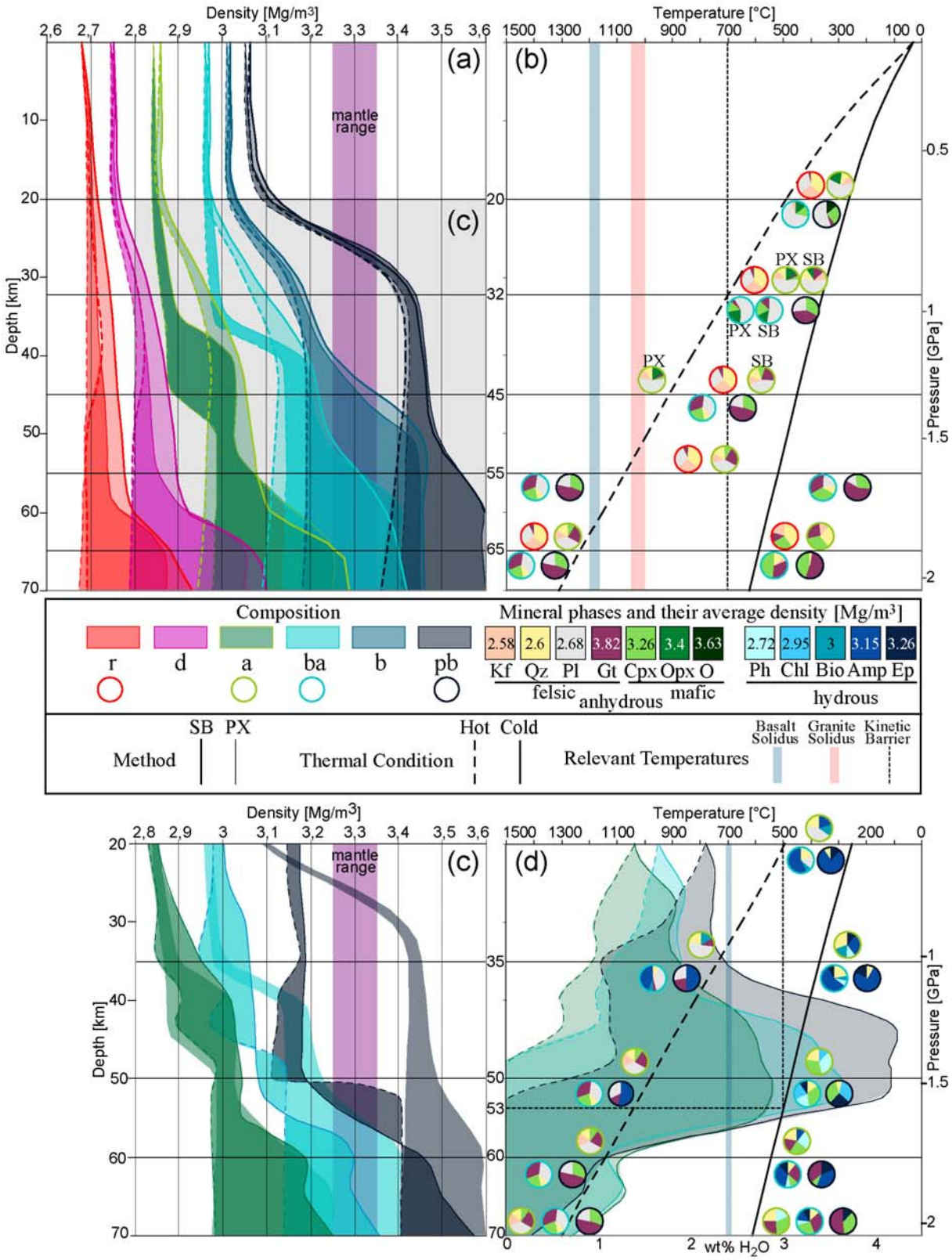

Fig. 3.2. Results of extensive petrophysical modelling for six selected samples (Fig. 3.1, Table 1) under anhydrous conditions in (a) and (b), and for andesite, basaltic andesite and picro-basalt under H_2O-saturated conditions in (c) and (d). The legend in between these figures shows: Colours representing each composition (labels as in Fig. 3.1) for density profiles of (a) and (c) and the border of pie diagrams depicting mineral

assemblages in (b) and (d); Colours representing mineral phases composing these assemblages (Kf potassic feldspar, Qz quartz, Pl plagioclase, Gt garnet, Cpx clinopyroxene, Opx orthopyroxene, O Olivine, Ph phengite, Chl chlorite, Bio biotite, Amp amphibole (including glaucophane), Ep epidote (including zoisite)) with values of average normative density after Hacker and Abers [2004]; Thermodynamic method applied: SB thick line is Sobolev and Babeyko [1994] and PX thin line is Perple_X [Connolly, 1990]; Thermal conditions: dashed-line is hot conductive geotherm defined (see text) by surface heat flow of 80 mW/m^2, bold-line is cold conductive geotherm defined by surface heat flow of 45 mW/m^2; Some relevant temperatures: dry [Katz et al., 2003] and wet [Schmidt and Poli, 1998] basalt solidus (light blue) and dry granite solidus [Holland and Powell, 2001] (light red), imposed kinetic barrier (dotted line). The purple "mantle range" in (a) and (c) was estimated from Poudjom Djomani et al. [2001], Jull and Kelemen [2001] and Kelly et al. [2003]. Light colouring of ranges in (c) is from anhydrous results of (a). (d) includes wt% of H_2O (bottom x-axis) contained in hydrous minerals. In the case that for a given composition the mineral assemblages calculated along hot and cold geotherms do not differ by more than 5 vol% in some phase, then pie diagrams in (b) and (d) are located between the curves for hot and cold geotherms. If differences are more than 5 vol%, then pie diagrams are plotted outside these curves.

At 40 km depth, PX density profiles for the basaltic andesite composition and the cold profile for the andesite join the density range estimated by SB, since mineral assemblages calculated by both methods coincide. At 45 km depth, differences less than 0.02 Mg/m^3 (0.6%) can be identified between the hot density profiles calculated by both approaches. The exception is the hot andesite profile of PX that remains at a density of 2.85 Mg/m^3 (same value observed in the upper crust), as the phase proportions stay constant with respect to that at 32 km depth. Despite the exception of the hot andesite profile, mineral assemblages calculated by both methods at the base of the lower crust (45 km) contain greater amounts of garnet than at 32 km depth, with the basaltic andesite showing the highest garnet increment from 13% to 30%. The dramatic density increment of the basalt composition along the cold geotherm between 40 and 50 km, surpassing the mantle density range at 45 km depth, is related with the total consumption of plagioclase to form clinopyroxene+quartz, defining an eclogite metamorphic facies. This phase change, and the consequent divergence between hot and cold density profiles, occurs only at lowermost crustal depths for the rest of the studied compositions, suggesting that it should be triggered by the anomalous geochemistry of this basalt (Table 1, Fig. 3.1). In particular, high concentrations of CaO and MgO and high values of Mg# coupled with low alkalis and ASI promote the formation of diopside at the expense of plagioclase.

3.4.1.3.Lowermost crust

Mineral proportions in granulite facies calculated by both approaches along the hot geotherm do not change below 45 km depth. A thermal expansion for temperatures between 900°C and 1300°C produces a slight density decrease (less than 0.6% at 70 km depth) along the hot lowermost crust with respect to values estimated in the lower crust. Densities calculated by both methods agree with each other into the tolerance range of 1%. All

compositions but the picro-basalt reach densities lower than the mantle range at the base of a hot crust. As for the rest of the crustal column, lowermost crustal densities seem to be positively correlated with the silica content of the constituent rocks. Note that in Fig. 3.2b dry solidus temperatures for granites and basalts are intersected by the hot geotherm at depths of 50 and 60 km, respectively; the deep portion of the hot lowermost crust could contain some silicate melt that should reduce the densities estimated here. This effect is evaluated later.

Mineral proportions formed by acidic to intermediate compositions do not differ between the hot and cold geotherm at 55 km depth. Thus, density differences up to 0.1 Mg/m^3 (~3.5%) between both thermal situations are due to the 600°C temperature divergence at that depth. In contrast, cold basic compositions form mineral assemblages with greater amounts of garnet and clinopyroxene and less plagioclase than their hot counterparts. This thermally-driven divergence of mineral assemblages leads to a density increment of 3% along the cold geotherm for the basaltic andesite and picro-basalt, implying a density difference of ~0.15 Mg/m^3 (~4.5%) between their hot and cold profiles at 55 km depth. The cold density profile of the basaltic andesite intersects the center of the mantle range at this depth.

Along the deeper part of the cold lowermost crust, the analysed compositions form eclogites dominated by garnet-clinopyroxene assemblages and with amounts of quartz and K-feldspar increasing with silica content. They differ notably from the plagioclase-bearing granulites formed along the hot thermal gradient. The divergence between hot and cold density profiles is complete at 65 km depth, where a density difference as high as 0.3 Mg/m^3 (~10%) can be attained. These large variations are primarily driven by differences in the mineral assemblages, but Moho temperatures for the hot crust are 700°C higher than for the cold thermal situation, producing a maximum expansion of the assemblages that further reduces their densities.

3.4.2. Empirical relationships between density and silica content under anhydrous conditions

Results presented for compositions analysed in the previous section indicate that silica content plays the primary role in controlling the density of rocks formed under anhydrous conditions. The same conclusion has been suggested by Sobolev and Babeyko [1994] on the basis of thermodynamical calculations performed for six crustal compositions similar to those presented in Table 1 but for a broad PT space. These authors also argued for a compositional control on seismic velocities, something confirmed by Behn and Kelemen [2003] who used PX with the database of Holland and Powell [1998] under anhydrous conditions to find that

variations of wt% SiO_2 along the composition space defined by more than 18,000 naturally occurring (meta)igneous rocks control variations in their seismic velocities. This is because variations of other major elements are strongly coupled with that of SiO_2 along the differentiation pattern of a magmatic arc (Fig. 3.1).

In an attempt to further explore this observation, densities were calculated at four critical depths using SB from the 55 compositional analysis plotted in the diagrams of Fig. 3.1. Considering that densities are constant up to 20 km depth (Fig. 3.2a), values calculated at surface conditions characterize those expected for the upper crust. Since the divergence of mineral assemblages and densities between those calculated along hot and cold geotherms occurs deeper than 35 km (Fig. 3.2a), a geothermal gradient in between these extremes (*Qs* = 65 mW/m^2) was used to compute densities at that depth. Values at 35 km depth characterize the pressure-controlled density increment occurring along the shallow section of the lower crust with respect to upper crustal densities. Note that values calculated by SB for compositions with SiO_2 concentrations between 50 and 60 wt% have to be considered with caution because PX densities for andesite and basaltic andesite compositions in this depth range are up to 3.5% lower than those obtained by SB (Fig. 3.2a). Values calculated at lowermost crustal depths (50 and 65 km) attempt to quantify the divergence in density profiles between hot and cold situations observed for basic compositions at 50 km depth, which is complete at 65 km for all compositions analysed in Fig. 3.2a. The results of these calculations are shown in Fig. 3.3.

A remarkably good inverse correlation can be recognized between silica content and calculated densities for all analysed PT conditions. Correlation factors of linear and power-law regressions are better than 0.85. Most of the dispersion impairing the density-silica correlation occurs along the basic compositional spectrum, as expected from the chemical variability of compiled analysis with SiO_2 content lower than 52 wt% (Fig. 3.1). Some rocks formed from basaltic compositions have densities at the Earth surface reaching that of the lithospheric mantle (Fig. 3.3a). For this reason, such rocks are found in the field in rare lower crustal sections exposed by exceptional tectonic processes (ophilite obduction, continental collision) or as xenoliths carried up to the surface by low density lavas. Taking this fact into consideration, surface densities were linearly regressed along SiO_2 contents higher than 52 wt% to characterize the relationship between these parameters at upper crustal levels. Fig. 3.3b shows the density-silica correlation improves to a factor of 0.95.

The dispersion along basic compositions decreases with depth in the lower crust, but trends are generally better described by power-law regression lines.

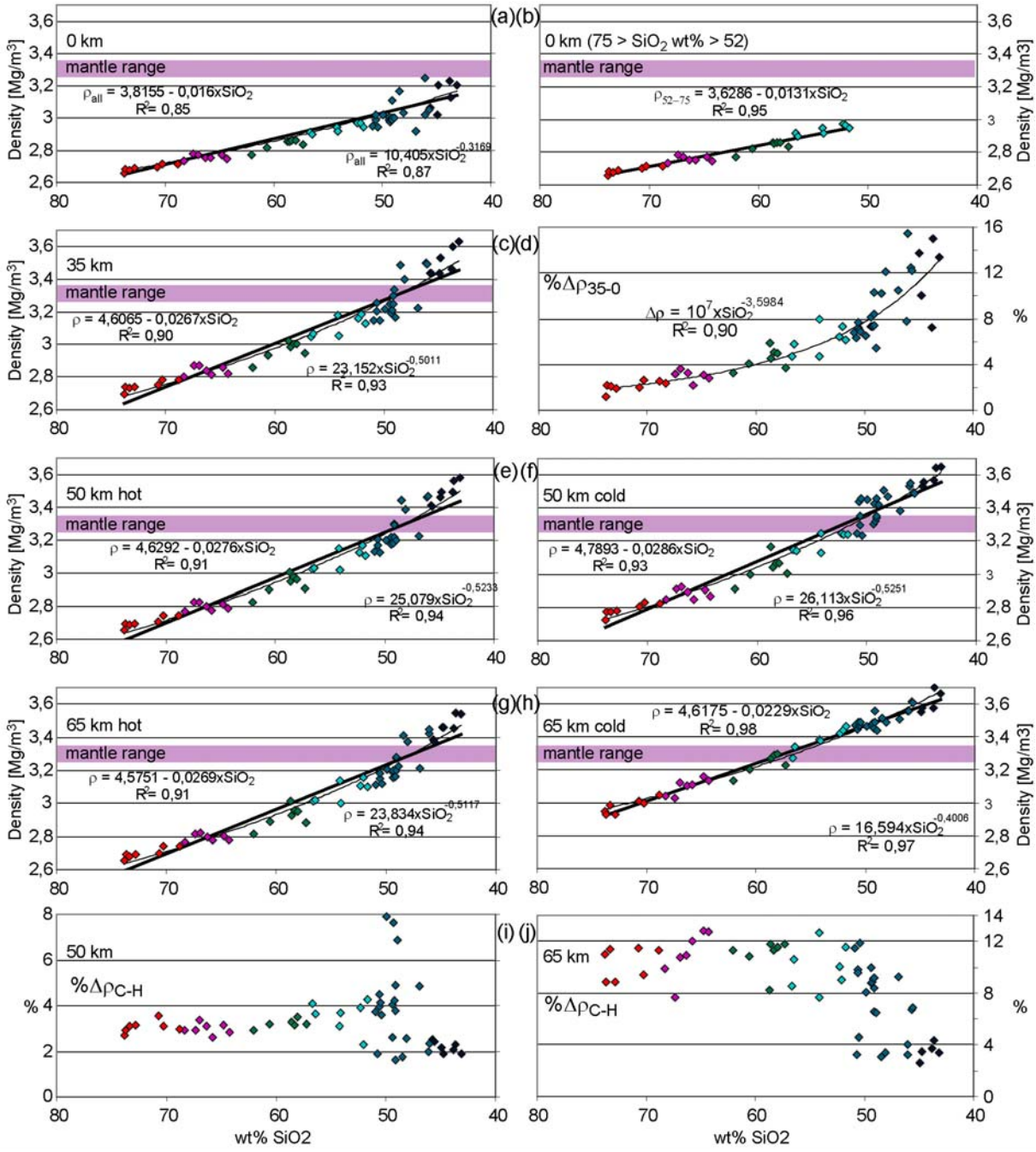

Fig. 3.3. Results of petrophysical modelling using the approach of Sobolev and Babeyko [1994] under anhydrous conditions for the whole compositional dataset. Calculated densities (a, b, c, e, f, g, h) and porcentage density differences (%Δρ; d, i, j) are plotted in the y-axis versus wt% SiO_2 in the x-axis. Colour coding distinguishes main compositional ranges as defined in Fig. 3.1. Mantle range as in Fig. 3.2. Empirical relationships between calculated parameters and silica content resulting from power-law (thin line) and linear (thick line) regressions are shown in diagrams (a) to (h) together with correlation factors (R^2). (a) 0 km depth (P=0 GPa, T=25°C); regressions considering all samples, some samples with less than 47 wt% SiO_2 have densities reaching the lower bound of the mantle range. (b) same as (a) but only linear regression and for samples with silica content between 52 and 75 wt% SiO_2; note that the density-silica correlation improves from a correlation factor of 0.85 in (a) to 0.95 in (b). (c) 35 km depth (P=1 GPa, T=550°C); most samples with less than 49 wt% SiO_2 have densities higher than the mantle range. (d) Percentage density difference between densities calculated at 35 and 0 km depth ($\%\Delta\rho_{35-0}$); values increase exponentially with decreasing silica content. (e) 50 km depth (P=1.4 GPa) along hot geotherm (T=960°C); densities change insignificantly compared with (c). (f) 50 km depth (P=1.4 GPa) along cold geotherm (T=500°C); samples with less than 52 wt% SiO_2 are at least as dense as the mantle. (g) 65 km depth (P=1.9 GPa) along hot geotherm (T=1250°C); densities change insignificantly compared with (c) and (e). (h) 65 km depth (P=1.9 GPa) along cold geotherm (T=570°C); samples with less than 58 wt% SiO_2 are at

least as dense as the mantle. (i) 50 km depth, percentage density difference between densities calculated along hot (e) and cold (f) geotherms ($\%\Delta\rho_{C-H}$); samples higher than 52 wt% SiO_2 show constant values near 3%, basic compositions have a large dispersion between 2 and 8%. (j) same as (i) but at 65 km depth; samples higher than 52 wt% SiO_2 show a higher dispersion than in (i) and $\%\Delta\rho_{C-H}$ values between 8 and 13%, basic compositions have a weak positive correlation with silica content.

This somehow mimics the non-linear trends of Fig. 3.1, indicating that variations in the concentration of other major elements modulates the primary control of silica. The trend of calculated densities against silica content at 35 km depth (Fig. 3.3c) is steeper than that observed at surface conditions. This indicates that the magnitude of the density increment along the lower crust is inversely correlated to SiO_2. This is quantified in the diagram of Fig. 3.3d, where the percentage increase of densities calculated at 35 km depth with respect to those on the Earth surface is plotted against wt% SiO_2. A power-law regression with an exponent of high absolute magnitude (-3.5984) fits the results well (R^2=0.9) and shows that rocks formed from compositions and PT conditions typifying the upper crust should be significantly denser (2-4%) if they are buried at lower crustal depths, but also that the magnitude of this effect increases exponentially with decreasing acidity. Basalts surpassing the mantle density range at 35 km show a dramatic density increment with respect to calculated values at the surface, being higher than 10% and, for some of the compositions with high alumina, as large as 16%.

The results obtained at 50 and 65 km depth along the hot geotherm are almost the same as observed at 35 km depth because granulite assemblages and, therefore, density profiles remains constant downward in the hot lowermost crust (Fig. 3.2a and b). The divergence occurring at 50 km depth in mineral proportions and densities calculated between the hot and cold thermal gradient (Fig. 3.2) implies that cold densities are significantly higher than those calculated under hot conditions (compare Figs. 3.3e and 3.3f). However, note that in Fig. 3.3i the magnitude of this density divergence ($\%\Delta\rho_{C-H}$) remains almost constant at ~3% along the compositional range between rhyolite and basaltic andesite, but shows a greater dispersion for basic compositions. In particular, basalts similar to that analysed in Fig. 3.2 present values of $\%\Delta\rho_{C-H}$ as high as 8%, whereas those having lower concentration of SiO_2, but normal contents of alumina and magnesium, commonly show density divergences near 2%. This suggest that the effect of temperature on the density of basic lowermost crustal rocks, namely their densification with decreasing temperatures, is strongly modulated by second-order variations of major elements away from the main trends defined against silica content. Although this seems to be true at 50 km depth, note that only 15 km deeper along the cold lowermost crust (Fig. 3.3h), the density of dense eclogite assemblages are very well

correlated with their silica content along a linear trend having a correlation factor of 0.98. This observation indicates that in a cold basic lowermost crust a chemical diversity like that depicted in Fig. 3.1 would have a minor effect on the primary control exerted by the concentration of SiO_2 in determining the density of eclogitic rocks. This is reflected in $\%\Delta\rho_{C-H}$ values calculated at 65 km depth (Fig. 3.3j) that, although with a greater dispersion than those at 50 km along the acidic to intermediate compositional range, have a positive correlation with silica content in the basic extreme.

If the compositional structure of active continental margins were to be defined by the differentiation trend depicted by the samples analysed in this study, then the empirical relationships presented in Fig. 3.3 could help to constrain the density range of anhydrous rocks along the entire crustal depth range using only the wt% SiO_2 of compositions expected to represent different crustal levels as a predictor. Significant differences in results obtained by SB and PX for intermediate compositions impose some restriction to the use of such relationships in the depth range of the lower crust (20-45 km) and compositional range of 50-60 wt% SiO_2. In particular, the density-silica correlation at 35 km depth presented in Fig. 3.3c could overestimate the density of rocks with intermediate compositions by 0.1 Mg/m^3 (~3.5%). The results presented next indicate that these relationships might also hold for hydrous crust under some specific conditions.

3.4.3. H_20-saturated crust

Fig. 3.2c compares the density ranges computed by PX under anhydrous conditions for three compositions typifying the lower crust (andesite, basaltic andesite and picro-basalt) against those obtained by the same approach imposing a complete water saturation in the thermodynamic system. The compensated Redlich-Kwong equation of state for H_2O of Holland and Powell [1991] was used during the thermodynamic calculations. Under H_2O-saturated conditions, water is always available to be absorbed and incorporated by hydrous silicates in mineral assemblages. It is assumed a full occupancy of OH sites in minerals and hence the water contents incorporated in the assemblages are maximum values. The kinetic barrier was reduced to 500°C because of the enhanced reactivity expected under water-saturated conditions. Calculations were performed deeper than 20 km depth, the kb-depth along the hot geotherm, because anhydrous calculations demonstrate that density values do not change within the upper crust. 500°C is intersected by the cold geotherm at 53 km (Fig 3.2d). Fig. 3.2d shows thermal gradients along with calculated mineral assemblages, and

includes ranges of H_2O (wt%) contained in hydrous mineral phases composing these assemblages.

3.4.3.1.Lower crust

Densities calculated from mineral assemblages formed by andesite and basaltic andesite compositions at 20 km depth are equivalent (within 1% uncertainty) to that computed at the same depth under dry conditions. Both compositions build amphibole-biotite tonalities, having less than 33% hydrous minerals for the andesite (with equal proportions of amphibole and biotite) and more than 60% amphibole for the basaltic andesite. Densities calculated under dry and wet conditions are similar because the average normative densities (hereafter ρ_{an}) for amphibole and biotite lie in between those of pyroxenes and feldspars (see legend of Fig. 3.2), phases that are totally or partially absent under water-saturated conditions (Fig. 3.2d). The density of the amphibolite formed by the picro-basalt is 3.15 Mg/m^3, significantly higher (0.05 Mg/m^3, ~1.5%) than its anhydrous counterpart at 20 km depth. This density value is that of an average amphibole, the mineral forming more than 80% of the calculated assemblage. The weight percent of water retained in the assemblages at 500°C and 20 km depth (0.6 GPa) are respectively 1.45%, 1.6% and 2.25% for andesite, basaltic andesite and picro-basalt compositions, indicating that H_2O contained in hydrous minerals increase with decreasing silica and increasing alumina.

With increasing depth in the lower crust, density ranges for andesite and basaltic andesite compositions are broader than those calculated under anhydrous conditions but remain around values estimated at 20 km depth. The density range of rocks formed from a water-saturated andesite composition is almost identical to that observed under dry conditions. This is because anhydrous minerals having ρ_{an} in the extreme of the density range (orthopyroxene and feldspars, see Fig. 3.2) are replaced by quartz and hydrous minerals that have densities in between these bounds. This replacement occurs in different proportions for different thermal conditions, but in a way that the final density of hydrated assemblages always equals the density of the assemblages formed under dry conditions (see discussion). A temperature difference of 350°C at 35 km depth generates a density difference up to 0.1 Mg/m^3 (~3%) between hot and cold density profiles of andesite and basaltic andesite. This difference is due to the decreasing amount of water accepted by mineral assemblages along the hot geotherm, where ~50% plagioclase and up to 5% garnet are formed. Along the cold geotherm, Na_2O, CaO and Al_2O_3 are combined with ~2 wt% H_2O (twice that accepted by hot assemblages) to form amphibole, micas (biotite and phengite) and epidote, all of them having

higher ρ_{an} than plagioclase. The divergence in mineral assemblages between hot and cold geotherms also occurs for the picro-basalt, however its density range is tight around a value of 3.15 Mg/m^3 because 50% garnet+plagioclase (in equal proportions) formed in hot conditions are equalled, in terms of density, by the same amount of amphibole+epidote±quartz along the cold geotherm.

The relevant density increment estimated to occur along the dry lower crust for basaltic andesite and picro-basalt compositions is absent under water-saturated conditions, mostly because dense garnet+pyroxene anhydrous granulites assemblages are replaced by amphibolites. In contrast with the anhydrous situation, rocks formed from a picro-basalt composition in a H_2O-saturated lower crust should be significantly less dense (by 0.15 Mg/m^3, 4.5%) than the mantle density range. Note that at 32 km depth, the wet solidus of basalt is intersected by the hot geothermal gradient and therefore the density of the lower crust could be further reduced by the presence of molten material.

3.4.3.2.Lowermost crust

At around 50 km depth (1.5 GPa) and equilibration temperatures of 950°C along the hot geotherm, no water is accepted by rocks formed from andesite and basaltic andesite compositions. The picro-basalt still retains 0.8 wt% H_2O, enough to allow the formation of 52% amphibole and to keep densities at relatively low values. Below 50 km depth, water is completely expelled from hot assemblages. Thus, mineral proportions and densities join those estimated along the dry lowermost crust and the picro-basalt surpasses the mantle density range. For this composition and the basalt, there is a depth range of 5 km thickness along which hot densities are higher than those calculated along the cold geotherm, which is related with the drastic change from amphibolite to dense granulite facies for the hot gradient whereas cold assemblages remain in low metamorphic grades.

In contrast with the situation observed along the hot geotherm, the amount of water contained in mineral assemblages along the cold geotherm is maximized at 50 km depth and temperatures corresponding to the kinetic barrier of 500°C. Rocks formed by andesite, basaltic andesite and picro-basalt absorb respectively 2.75, 3.6 and 4.15 wt% H_2O at this depth. Amphibole, which is a low water-consuming mineral (less than 2 wt% H_2O in its structural formula), is not a stable phase at these conditions and mineral assemblages comprise clinopyroxene, quartz, chlorite (a high water-consuming phase) and amounts of epidote and white mica increasing and decreasing respectively with decreasing silica. These rocks are intermediate between greenschist and amphibolite metamorphic facies. Increasing

equilibration temperatures at levels deeper than the kb-depth of the cold geotherm (53 km) gradually expel water from all assemblages, a phenomenon leading to the continuous downward density increase and the formation of increasing amounts of garnet, glaucophane and epidote (zoisite) at the expense of clinopyroxene and chlorite. The cold density profile of a picro-basalt intersects the mantle density range at 55 km depth, whereas that of a basaltic andesite intersects it near 60 km depth. However, densities along the deep and cold hydrous lowermost crust never reach values estimated under dry conditions because between 60 and 70 km depth, some 1 wt% H_2O is still accepted to form hydrous minerals. As for the rest of the crustal column, the density range of a water-saturated andesite composition is indistinguishable from that computed under anhydrous conditions. Along the cold lowermost crust this situation results from the replacement of anhydrous felsic minerals by phengite, both having similar ρ_{an}.

3.4.4. Quantifying the effect of partial melting

The hot geotherm used in this study reaches the dry solidus temperature of granites [Holland and Powell, 2001] and basalts [Katz et al., 2003] at depths of 53 and 63 km, respectively (Fig. 3.2b), whereas the wet solidus of basalts [Schmidt and Poli, 1998] is intersected near 35 km depth (Fig. 3.2d). Therefore, it is expected that the deep and hot continental crust, mostly under hydrous conditions, could contain significant amounts of partially molten material. The retention of magmas into a network of co-genetic residues in a MASH zone could reduce the average density of the arc roots, since silicate liquids are notably lighter than solid rocks [e.g. Lange and Carmichael, 1990]. It is then relevant to quantify the reduction of lower crustal density generated by a given proportions of retained melt (F). A linear relationship between density of solid phases (ρ_{solid}) and that of melt (ρ_{melt}) is used to calculate the average density of a MASH zone [see also Schmitz et al., 1997]:

$$\rho_{MASH} = \rho_{solid}(1-F) + \rho_{melt}F$$

Densities of anhydrous melts of basaltic (2.95 Mg/m^3) and andesitic (2.65 Mg/m^3) compositions were extrapolated from diagrams presented by Lange and Carmichael [1990] for a pressure of 1.5 GPa (~50 km depth) and temperatures of 1200°C and 1000°C, respectively. Because subduction-related magmas likely contain dissolved water [e.g. Gaetani et al., 1993] a value of 0.075 Mg/m^3 was subtracted from values above to simulate the effect

produced by 1 wt% H_2O in decreasing the density of hydrous silicate melts [Ochs and Lange, 1999]. Results of these calculations are shown in Fig. 3.4.

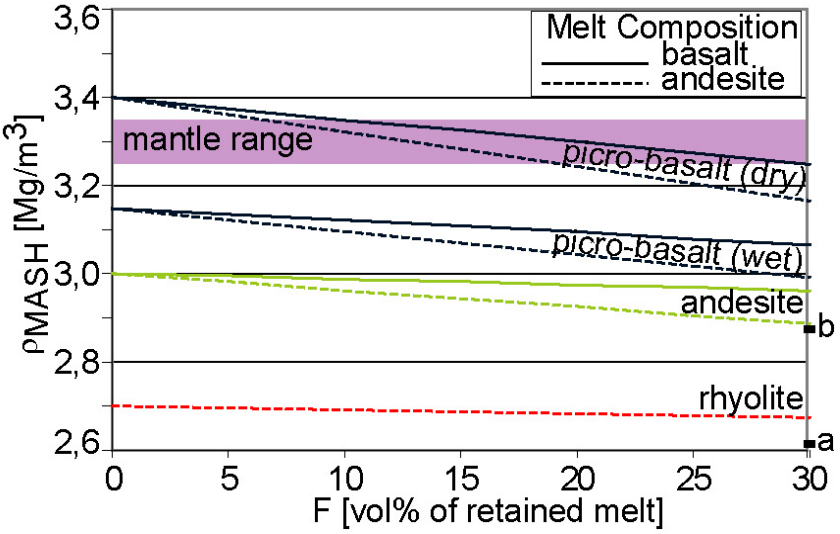

Fig. 3.4. Average density of a MASH zone (ρ_{MASH}, see text for definition) formed by a mixture of solid rocks and a given volume percent of retained melt (F). Solids are picro-basalt dry (anhydrous), picro-basalt wet (H_2O-saturated), andesite and rhyolite. Colours and mantle range as in Fig. 3.2. Solid densities (F=0) are those calculated along the hot geotherm at 50 km depth (Fig. 3.2). Melt compositions are basalt (bold line) and andesite (dotted line). Melt densities (F=100; dots labelled a=andesite and b=basalt on the right y-axis) were estimated as described in the text.

The density reduction of crustal columns due to a retention of melt at lower crustal depths reaches a maximum for dense mafic garnet granulites formed from a picro-basalt composition under dry and hot conditions. That is expected because of the large density contrast between these rocks and silicate melts. As this contrast decreases, either because solids are more acidic and lighter or because anhydrous mafic granulites are replaced by amphibolites under water-saturated conditions, so does the melt-driven density reduction. The presence of partially molten material with an intermediate to acidic composition (density for rhyolitic magmas after Lange and Carmichael [1990] differ little from those of andesitic melts) has no appreciable effect on resulting average densities if the crust has this same composition (Fig. 3.4).

In order to reduce the average density of a lower crustal MASH zone with a picro-basalt composition under anhydrous conditions to values characteristic of the mantle range, it is necessary to retain ~12 vol% of trapped basaltic melt. If this melt were andesitic in composition, less than 8 vol% should be enough to make a mafic dry granulite lower crust neutrally buoyant with respect to the mantle. These values are lower than estimates proposed from interpretation of geophysical data for the lower crust of continental plateaus (15-25 vol% partial melt: e.g. Schilling et al. [1997], Schmitz et al. [1997] and Schilling and Partzsch

[2001]), which should be considered an upper limit for normal degrees of partial melting in active magmatic arcs.

3.5. Discussion

3.5.1. Contrasting effect of water saturation on lower crustal rocks

PX calculations under hydrous conditions (Fig. 3.2c and d) demonstrate that forcing a complete water saturation for the formation of mineral assemblages has contrasting effects on the density ranges calculated for compositions representative of the lower crust. This effect is a strong density reduction with respect to dry values for rocks formed from a picro-basalt composition at lower crustal levels (30-50 km depth). This reduction makes such rocks, which under dry conditions are significantly denser than the underlying mantle, 0.15 Mg/m^3 (4.5%) lighter than the mantle density range. In contrast, rocks formed from an andesite composition have the same density range (within 1% uncertainty and without considering differences between PX and SB under anhydrous conditions) along the entire crustal column both for dry and wet conditions. The basaltic andesite composition shows a behaviour in between these extremes, with a significant density reduction occurring in the deep portion of the lower crust.

These disparities in the response to the saturation in water reside in the increasing amount of H_2O that can be retained by rocks with increasing Al_2O_3/SiO_2 ratios and in the way anhydrous minerals are replaced by hydrous phases for different compositions. As shown in Fig. 3.2d, the picro-basalt can absorb more water than the andesite for all PT conditions, with differences of ~0.5 wt% along the hot geotherm and up to 1.5 wt% at the base of the cold lower crust. At 35 km depth and for hot conditions, this results in assemblages comprising hydrous minerals in proportions of 50% for the picro-basalt and only 15% for the andesite, whereas along the cold geotherm they increase to 90% and 66%, respectively (Fig. 3.2d). The cause for the great amount of water being incorporated in mineral assemblages formed from a picro-basalt is likely the same as that controlling the formation of dense rocks under anhydrous conditions; high Al_2O_3/SiO_2 ratios (0.42) characteristic of this composition together with high concentrations of CaO, FeO and MgO promotes the formation of great proportions of mineral phases having similarly high values, i.e. garnets ($Al_2O_3/SiO_2 \approx 0.55$) under dry conditions and amphiboles ($Al_2O_3/SiO_2 \approx 0.45$) for wet systems. The replacement of anhydrous granulite assemblages comprising more than 75% garnet+clinopyroxene (Fig. 3.2b) by amphibolites produces the strong density decrease observed for the picro-basalt, because an average amphibole is ~10% lighter than the average of those anhydrous minerals.

This change in mineral assemblages and subsequent reduction of density can be appreciated in the following reaction:

$$(Ca, Fe, Mg)_3Al_2Si_3O_{12} + 2Ca(Fe,Mg)Si_2O_6 + H_2O \rightarrow Ca_2(Mg,Fe)_4(Al,Fe)Si_7AlO_{22}(OH)_2$$

garnet (ρ_{an}=3.82 Mg/m^3) + 2 clinopyroxene (ρ_{an}=3.26 Mg/m^3) + H_2O → amphibole (ρ_{an}=3.15 Mg/m^3)

In contrast, a hydrated rock with an andesite composition cannot retain too much water because its low Al_2O_3/SiO_2 ratio and low concentration of CaO+FeO+MgO precludes the saturation in amphibole or other mafic hydrous minerals (e.g. epidote). The relatively high concentration of alkalis favours the incorporation of water in micas (biotite and phengite) having ρ_{an} between the extremes of those minerals forming dry andesitic assemblages (orthopyroxene and feldspars, Fig. 3.2b). This replacement can be exemplified by the reaction:

$$3(Mg,Fe)_2Si_2O_6 + 2KAlSi_3O_8 + 2H_2O \rightarrow 2K(Mg,Fe)_3AlSi_3O_{10}(OH)_2 + 6SiO_2$$

3 o-px (ρ_{an}=3.4 Mg/m^3) + 2 K-fspar (ρ_{an}=2.6 Mg/m^3) + 2H_2O → 2 bio (ρ_{an}=3 Mg/m^3) + 6 qtz (ρ_{an}=2.6 Mg/m^3)

Therefore, the density range of rocks with an andesite composition tends to be almost identical under dry and water-saturated conditions.

These results have as a practical consequence that the empirical relationships between density and silica content proposed above for rocks formed under anhydrous conditions could also be used to constrain the density range of hydrous rocks having intermediate to acidic compositions. Water-saturated calculations for the rhyolite (not shown here) indicate that rocks formed from this composition would absorb some 1 wt% H_2O at PT conditions maximizing the water content of intermediate to basic compositions (Fig. 3.2d; T=500°C, P=1.5 GPa) and less than 0.5 wt% H_2O would be absorbed along the hot geotherm. This could result in the replacement of minor amounts of K-feldspar and quartz by white mica and insignificant changes in calculated densities. Thus, the effect of water in changing the density of acidic to intermediate rocks with respect to their anhydrous counterparts is minimal, as is the effect of retained melts at lower crustal levels (Fig. 3.4). Therefore, rock densities in this compositional range could likely always be predicted from their silica content. That is not the case for basic compositions, which respond to a saturation in water and presence of partially molten material with a dramatic decrease in density.

3.5.2. Buoyancy of hydrated, mafic lower crust

If the lower crust were effectively flooded by large amounts of water, allowing saturation of the system with H_2O, then its density would likely be much lower than the underlying mantle. This has the important consequence that lower crustal residues, which under anhydrous conditions are gravitationally unstable and able to sink into the mantle, could be positively buoyant in a water-saturated environment, tending to stay attached to the continental crust. It is then relevant to discuss whether H_2O-saturated conditions could be reached in natural systems.

Probably the only places where lower crustal water-saturation is a plausible scenario are those sites where most of the continental crust has been likely created, i.e. subduction zones [e.g. Rudnick, 1995; Tatsumi, 2000; Carlson et al., 2005]. The oceanic lithosphere transports between 3 and 6 wt% H_2O before entering the trench [e.g. Hacker et al., 2003a; Forneris and Holloway, 2003; Iwamori, 2004]. Although most of this water is released by dehydration reactions below the forearc region, sufficient amounts remain in the slab under the volcanic arc to trigger hydrous melting of mantle wedges [Hacker et al., 2003b; Katz et al., 2003; van Keken, 2003]. Several authors have pointed out that the further evolution of mantle-derived melts at the base of magmatic arcs might occur in the presence of water in order to generate a calcalkaline differentiation trend [Hildreth and Moobarth, 1988; Sisson and Grove, 1993; Gaetani et al., 1993; Grove et al., 2003]. Amphibole crystallizes in most of the experiments carried out from hydrated basaltic to basaltic andesitic liquids [e.g. Moore and Carmichael, 1998; Münthener et al., 2001; Grove et al., 2003 and reference therein]. In addition, amphibolites and amphibole-rich gabbros are common rock types found along active continental margins and in xenoliths transported to the surface by arc lavas [Costa et al., 2002 and reference therein] and are thought to be fractionation products from parental magmas of subduction-related volcanic series [Dungan and Davidson, 2004; Sellés et al., 2004].

These arguments support the idea that the lower crust of active magmatic arcs is in a state of, at least partial, water saturation. Nevertheless, lower crustal xenoliths and exposed terrains also contain significant proportions of anhydrous granulites and eclogites [e.g. Rudnick and Fountain, 1995; Ducea, 2002; Yoshino and Okudaira, 2004], suggesting that lower crustal sections are likely formed by a mixture between these two end-members. A mechanical mixing of 45 vol% amphibolites (3.15 Mg/m^3) with dense anhydrous mafic assemblages (3.42 Mg/m^3) can reduce the average density of a (picro-)basaltic lower crustal column (30-50 km depth range) to values comparable to the lithospheric mantle (3.3 Mg/m^3).

This generates a neutral buoyancy with respect to the underlying mantle and protects the mafic lower crust from convective removal. An additional density reduction due to the retention of silicate melts in lower crustal MASH zones can further increase the buoyancy of (ultra)mafic, basaltic lower crust.

The upward transport of water from the dehydrating slab and partial melting of the mantle wedge should also reduce the density and viscosity of the mantle [e.g. van Keken, 2003], decreasing the relative buoyancy of the lower crust and promoting the growth of gravitational instabilities [Jull and Kelemen, 2001]. In the extreme that the sub-arc mantle would contain 20 vol% of fully serpentinized peridotite (the value seismically estimated for hydrated mantle forearcs by Carlson and Miller, [2003]) with a density of 2.7 Mg/m^3 [Hacker and Abers, 2004], and 5 vol% of basaltic melt with one weight percent water and a density of 2.9 Mg/m^3 [Lange and Carmichael, 1990; Ochs and Lange, 1999], the mantle density could reduce from an average of 3.3 Mg/m^3 to 3.16 Mg/m^3. In this extreme case, a mafic lower crust composed of residues with a picro-basalt composition must have formed under complete water-saturated conditions in order to remain neutrally buoyant with respect to the underlying mantle.

Whatever the case, these results suggest that ultramafic residues left at the base of magmatic arcs with normal crustal thickness of 40-45 km [Christensen and Mooney, 1995; Rudnick and Fountain, 1995] might not always be forced to collapse into the underlying mantle, as proposed by Jull and Kelemen [2001], Münthener et al. [2001] and Ducea [2002]; they could be retained in a hydrated lower crust in the form of mafic amphibolites containing some volume percent of basaltic melt.

These rocks might be seismically hidden in the lower crust, since seismic velocities are also reduced by the formation of hydrated minerals and the presence of partial melting. During the thermodynamic calculations carried out in this study, P-wave velocities (Vp) were computed along with densities. As shown in Fig. 3.5, the Vp range of anhydrous rocks formed within the lower crust (30-50 km depth) from a picro-basalt composition is around 7.8 km/s, but this range is reduced to values of 6.9-7.2 km/s for water-saturated calculations. This hydrous Vp range is comparable to P-wave velocities characteristic of a basaltic andesite composition under dry and hot conditions. This suggests that estimates of crustal composition from seismic velocity models considering only anhydrous minerals for depths higher than 30 km [e.g. Christensen and Mooney, 1995; Rudnick and Fountain, 1995; Gao et al., 1998] could underestimate the basicity of the continental crust, a phenomenon that helps to explain disagreements with estimates of global crustal compositions resulting from surface heat flow

models [McLennan and Taylor, 1996]. This hypothesis must be systematically explored in order to evaluate its impact on current estimates of global crustal composition and models of crustal growth.

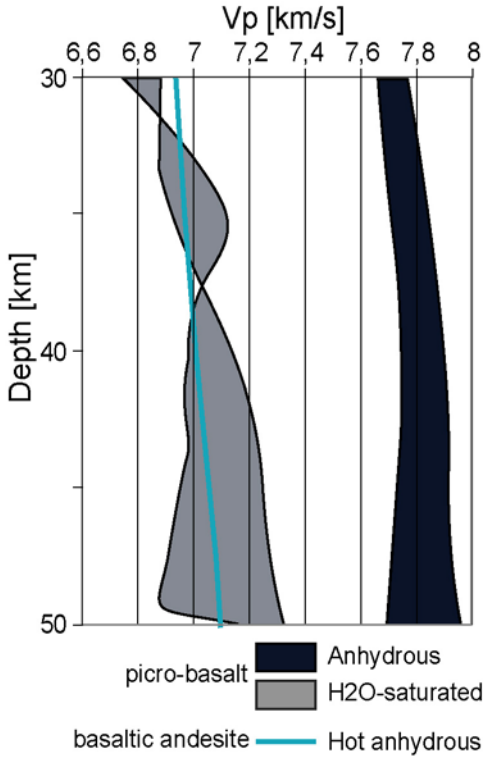

Fig. 3.5. P-wave seismic velocity (Vp, x-axis) between 30 and 50 km depth (y-axis) calculated during petrophysical modelling. Vp ranges result from calculations along hot and cold geotherm for anhydrous picro-basalt (dark grey), H_2O-saturated picro-basalt (light grey) and hot anhydrous basaltic andesite (light blue line). Vp values around 7.8 km/s for picro-basalt composition under anhydrous conditions reduce to 6.9-7.2 km/s under water-saturated conditions. This latter range is similar to Vp values for a basaltic andesite under hot anhydrous conditions.

3.5.3. Scenarios for the gravitational instability and removal of dense lowermost crust

Results presented in this contribution restrict the potential loss of lower crustal roots of active continental margins to particular conditions. Beneath active magmatic arcs, continuous removal of lower crustal material may occur in the form of small-scale Rayleigh-Taylor instabilities [Jull and Kelemen, 2001; Dufek and Bergantz, 2005] that drag down dense residues left at the base of MASH zones. As supported by arguments discussed before, these zones might be hot, partially saturated with water and retaining some amounts of molten material. The base of a MASH zone must be deeper than 45-50 km in order to expose mafic residues to PT conditions where water cannot be incorporated into light hydrous minerals and the density contrast between melt and solids can drive the extraction of the melt fraction. In this scenario, dense granulites are formed in an anhydrous system (Fig. 3.2d) and their

densities can be predicted from the empirical relationships previously proposed. Figs. 3.3e and 3.3g show that residues formed deeper than 50 km below a hot arc are expected to be negatively buoyant with respect to the mantle only if their silica contents are not higher than 49 wt%. Such dense mafic residues at the base of a weak arc have great potential to be removed by convective instabilities in some million years [Jull and Kelemen, 2001], mostly if they retain minor amounts of interconnected melt [Dufek and Bergantz, 2005].

The presence at the Earth surface of old arc roots, like the Kohistan and Tonsina sections [Miller and Christensen, 1994; Yoshino and Okudaira, 2004; DeBari and Coleman, 1989], demonstrate that mafic-ultramafic keels can remain attached to the crust several million years after they became extinct. Similarly, garnet-pyroxene xenoliths of Cretaceous age that are cogenetic with the felsic Sierra Nevada batholith and were captured by Miocene lavas [Ducea and Saleeby, 1998], attest for the preservation of the arc root underneath the Sierran batholith by more than 70 Ma after the extinction of the arc [e.g. Saleeby et al., 2003; Zandt et al., 2004]. Nevertheless, the absence of such xenoliths in Pliocene-Quaternary lavas and a robust body of seismic data [Zandt et al., 2004 and reference therein] indicate that the Cretaceous arc root is being foundered below the southern Sierra Nevada. Zandt et al. [2004] suggest that this process was triggered by a combination of factors that tend to reduce the density and viscosity of the mantle and increase the ambient strain rate, helping for the development of a convective instability.

Another mechanism for the loss of mafic lower crust from beneath active margins is the piecewise and presumably catastrophic delamination of large lowermost crustal and mantle blocks, after being converted to dense material due to burial and pro-grade metamorphism during orogeny [Bird, 1979; Kay and Kay, 1993; Houseman and Molnar, 1997; Moore and Wiltschko, 2004]. Thickening orogens along an active margin share their tectonic setting with the evolving magmatic arc, and hence might be characterized by a hot, wet and partially molten lower crust. Therefore, the same conditions inferred to favour the continuous convective removal of residues from the arc, hold also for the delamination of the orogenic lower crust: A crust thicker than 45-50 km and the existence of garnet granulites with silica content lower than 49 wt%. However, the retention of such dense rocks in a magmatic arc that is thickening, is limited by the development of fast convective instabilities below the threshold of 50 km depth. Thus, in order for catastrophic delamination of huge lower crustal blocks to take place, a tectonic thickening event shorter than the time-scale of evolving convective instabilities (1-10 My, see Jull and Kelemen [2001]) may be a prerequisite. Note, however, that this thickening cannot be too fast, otherwise the

amphibolite-to-granulite phase transformation might be kinetically delayed and a buoyant amphibolite-rich lowermost crust could be retained in a meta-stable situation. These restrictions converge with the scarcity of geological and geophysical evidence attesting for the lower crustal delamination of orogenic upper plates, which seems to be a relatively rare event [e.g Kay and Kay, 1993; Moore and Wiltschko, 2004].

This is in contrast with the syncollisional detachment of the lower continental plate colliding against an active margin, which is a common process resulting in the collapse of most collisional orogens [e.g. Leech, 2001; Moore and Wiltschko, 2004 and reference therein]. The reason of this difference resides, at least partially, in the contrasting thermal conditions expected for both plates before orogenic thickening. As noted by Moore and Wiltschko [2004], passive margins arrive at a collision zone with a cold thermal structure that, after being tectonically buried as they are dragged by the subducting slab, promotes both the negative buoyancy of mantle lithosphere with respect to the asthenosphere and the eclogitization and densification of lower crustal rocks (Fig. 3.2). Thus, the deep part of the lower plate is prone to detach from the buoyant upper crust along mechanically weak zones [Moore and Wiltschko, 2004]. Leech [2001] and Bjornerud and Austrheim [2004] pointed out that the phase changes from low-pressure metamorphic facies to eclogite might be kinetically impossible if fluids are not generously present to catalyse metamorphic reactions. This observation and results presented in Fig. 3.2c suggest a scenario where the only rocks that could surpass the mantle density at lowermost crustal depths are those formed in a hydrous system from compositions more basic than a basaltic andesite (SiO_2 < 52 wt%). If eclogitization of lower crustal rocks could occur under dry conditions, then the maximum content of silica necessary to produce eclogites denser than the mantle increases to 58 wt% SiO_2, namely an andesite composition (Fig. 3.3h).

3.6. Summary and Conclusions

This manuscript presents results of petrophysical modelling performed with the thermodynamical approaches of Sobolev and Babeyko [1994] and Connolly [1990, Perple_X] over 55 geochemical analyses that characterize calc-alkaline, subduction-related continental margins. Mineral assemblages equilibrated at pressure-temperature (PT) conditions along hot and cold conductive geotherms were extracted to calculate density profiles at *in situ* PT conditions down to 70 km depth. An extensive analysis under anhydrous equilibration conditions for six samples representative of the dataset, shows that results of both methods agree with each other, although some discrepancies exist for rocks with intermediate

compositions in the depth range 20 to 40 km. The approach of Sobolev and Babeyko [1994] was then used to calculate density values for the whole dataset at four critical depths and to regress these values against silica. The resulting regressions have correlation factors greater than 0.85, which indicate that densities are inversely correlated with wt% SiO_2 for all considered anhydrous PT conditions. These regression lines constitute empirical relationships that are useful for constraining the density range of anhydrous crustal rocks.

Perple_X was then used under water-saturated conditions. For intermediate to acidic compositions, the effect on density of water and retained melt is minimal, and the empirical density-SiO_2 relationships obtained under anhydrous conditions could also be applied to a wet, melt-containing crust with bulk silica content higher than 55-60 wt%. That is not the case for rocks formed from (ultra)basic compositions, which absorb large amounts of water via the formation of amphiboles, notably reducing their density with respect to the garnet-pyroxene assemblages formed under dry conditions.

These results were used to infer that lower crustal zones of melting, assimilation, storage and hybridisation (MASH zones after Hildreth and Moorbath [1988]) with (picro)basalt bulk composition at the base of subduction-related arcs of normal crustal thickness (<50 km), could be positively buoyant with respect to the mantle due to the presence of amphibole-rich zones and the retention of melts. These zones should have seismic velocities typical of anhydrous rocks of basaltic andesite composition and hence it is speculated that estimates of crustal composition based on seismic models [e.g Rudnick and Fountain, 1995; Christensen and Mooney, 1995] could underestimate the basicity of the continental crust.

Convective instabilities dragging down residues left at the base of magmatic arcs should take place only if the crust is thicker than 50 km, leading to the densification produced by the phase change from amphibolite to granulite. But, because of high temperatures, this is restricted to rocks more basic than 49 wt% SiO_2. The same conditions are necessary for the catastrophic delamination of the orogenic lower crust. This phenomenon has to be triggered by particular tectonic processes, during which the velocity of crustal thickening and the kinetic rate of metamorphic reactions should reach an equilibrium in order to thicken, dehydrate and generate the densification of the lowermost crust before small-scale and continuously evolving convective instabilities could remove it first. These restrictions help to explain why upper plate delamination events [e.g. Kay and Kay, 1993] seems to be less common than lower plate syncollisional detachment [e.g. Moore and Wiltschko, 2004], since these latter processes are promoted by the cold thermal structure carried by the passive margin

toward a collision zone and the water-assisted eclogitization of lower crustal rocks as acidic as 52 wt% SiO_2.

Results presented in this manuscript, namely the empirical relationships between density and silica content of meta-igneous rocks and the quantification of the effect produced by temperature, water content and retention of partially molten material on the density ranges of crustal sections, should help to design and interpret gravity models describing the density structure of continental margins and thermomechanical models dealing with their temporal evolution.

3.7. Acknowledgements

I wish to thank Friedrich Lucassen for getting me started with Perple_X, and Stephan Sobolev and Andrey Babeyko, who kindly supplied me with the updated version of their thermodynamic approach and guided me on its use. The continuous discussions with Andrey Babeyko, Ron Hackney and Daniel Sellés and the critical review they made of a first version of this manuscript, strongly improved the clarity and quality of this work. Suggestions made by the reviewers Rebecca Lange, Mihai Ducea and the associated editor James Tyburczy are greatly appreciated. This study is part of my Ph.D. thesis at the Freie Universität Berlin under the supervision of Hans-Jürgen Götze.